The EMBO Journal vol.10 no.5 pp.1159-1167, 1991

An upstream XylR- and IHF-induced nucleoprotein complex regulates the σ^{54}-dependent Pu promoter of TOL plasmid

Victor de Lorenzo[1], Marta Herrero, Martin Metzke* and Kenneth N.Timmis

GBF-National Research Centre for Biotechnology, 3300 Braunschweig, FRG and [1]Centro de Investigaciones Biológicas, CSIC, 28006 Madrid, Spain.

Communicated by K.N.Timmis

*Dedicated to the memory of our friend and colleague Martin Metzke, deceased August 1990

Transcription from promoter Pu of the upper catabolic operon of the *Pseudomonas putida* TOL plasmid which specifies conversion of toluene/xylenes to benzoate/toluates is activated by the TOL-encoded regulator XylR protein in the presence of substrates of the catabolic pathway and in conjunction with the σ^{54}(NtrA)-containing form of RNA polymerase. This regulatory circuit was faithfully reproduced in *Escherichia coli* in single copy gene dosage by integrating the corresponding controlling determinants into the chromosomes of several K12 derivatives by means of specialized transposons. *In vivo* monitoring of the activity of a *Pu-lacZ* fusion in *E.coli* strains with different genetic backgrounds demonstrated that integration host factor (IHF) is involved in Pu regulation and that hyperproduction of the XylR protein leads to a decrease of Pu activity in a manner in which deletion of the putative DNA-binding domain of the XylR does not impair its inhibitory effect when hyperproduced. One discrete IHF binding site and two potential XylR sites (consensus sequence 5′-TTGANCAAATC-3′), bracketted by short stretches of DNase I- hypersensitive bonds, were detected upstream of the transcription initiation site. A model accounting for the features found is proposed which includes the IHF-promoted looping of upstream XylR-DNA complexes so that they contact the σ^{54}(NtrA)-RNA polymerase bound at −12/−24 positions.

Key words: DNA bending/IHF/*Pseudomonas*/TOL plasmid/XylR

Introduction

Catabolism of toluene/xylenes by *Pseudomonas* strains carrying the TOL plasmid pWWO is determined by two plasmid-carried operons which encode the oxidative transformation of toluene/xylenes to the corresponding benzoate/toluates (upper operon) and the subsequent metabolism of the carboxylic acids via a *meta*-ring cleavage onto TCA cycle intermediates (*meta* operon). In response to the appearance of pathway substrates, both operons become coordinately transcribed. The complex regulatory circuit that controls transcription of the catabolic operons has been the subject of recent reviews (Harayama and Timmis, 1989; Ramos *et al.*, 1987; Nakazawa *et al.*, 1990). The mechanism of transcriptional control includes at least two TOL-borne regulators, XylS and XylR, the latter acting on the promoter of the upper operon (Pu) and on that of *xylS* (Ps) in conjunction with the σ^{54} (RpoN,NtrA)-containing form of the RNA polymerase (Köhler *et al.*, 1989; Inouye *et al.*, 1989).

Deletion analyses of Pu and XylS promoters (Holtel *et al.*, 1990; Inouye *et al.*, 1990) have revealed that, as is the case with other σ^{54}-dependent promoters (Buck *et al.*, 1987; Kustu *et al.*, 1989; Morett and Buck, 1988; Sasse-Dwight and Gralla, 1990), upstream activation sequences (UAS) are necessary for a full XylR-mediated induction by toluene and other pathway substrates. Sequence comparisons led Holtel *et al.* (1990) to propose a potential XylR-binding consensus UAS 5′-TGATGATTTGCTNAAATNCACNC-3′ which is repeated twice upstream of the transcription initiation site in the Pu promoter region (−176 to −170 and −138 to −122) and the Ps promoter region (−145 to −129 and −169 to −153). In addition, a role for the integration host factor (IHF) was suggested by the sequence similarity of the region between −62 to −27 of Pu and −89 to −54 of Ps with a functional IHF site at the NifA/ σ^{54} -dependent promoter P*nifH* (Santero *et al.*, 1989; Hoover *et al.*, 1990). In this paper, we examine the influence of IHF on Pu promoter activity *in vivo* and demonstrate its binding *in vitro* to Pu and Ps promoters. Furthermore, we identify by DNase I footprinting the sites of binding and the distribution of IHF and XylR interactions within the Pu promoter, which results in the formation of a nucleoprotein upstream complex.

Results

IHF influences Pu expression in vivo and binds strongly to Pu and weakly to Ps in vitro

Pu contains an IHF-binding consensus sequence 5′-WATCAANNNNTTR-3′ (Friedman, 1988; Yang and Nash, 1989) starting at position −56 from the transcription initiation site. Since IHF binds *in vitro* and activates P*nifH* (Santero *et al.*, 1989; Hoover *et al.*, 1990), and potential IHF sites are found also in other σ^{54}(NtrA)-dependent promoters (Holtel *et al.*, 1990; Hoover *et al.*, 1990; Gober and Shapiro, 1990), we were interested in determining its role, if any, in Pu regulation. In order to reproduce faithfully in *E.coli* all the regulatory elements involved in the control of Pu activity, we constructed two specialized transposons: (i) a mini-Tn*5* Sm/Sp::*Pu-lacZ*, which delivers into the chromosome of a target bacterium a *Pu-lacZ* fusion shielded transcriptionally upstream by an Ω interposon (Prentki and Krisch, 1984) and downstream by a T7 terminator and (ii) a mini-Tn*10* Ptt::*xylR/xylS*, which delivers in the same fashion a TOL-derived restriction fragment with *xylR* and *xylS* transcribed from their native promoters. The *Pu-lacZ* and *xylR/S* inserts were integrated in isogenic *himA*$^+$*himD*$^+$, *himA*$^-$*himD*$^+$ and *himA*$^+$*himD*$^-$ strains

(*himA* and *himD* encode the two IHF subunits) as described in the Materials and methods section and cultured in the presence of the Pu promoter inducer *p*-chlorobenzylalcohol, *p*-ClBA (Abril *et al.*, 1989). Figure 1 shows the result of an induction experiment which indicated a sharp decrease in Pu promoter activity in strains devoid of IHF.

In order to confirm the interaction of IHF and XylR with Pu suggested by the *in vivo* experiments, we set up gel retardation assays with soluble extracts from isogenic *himA*$^+$*himD*$^+$ and *himA*$^-$*himD*$^+$ strains transformed with pEZ6, a plasmid directing XylR overproduction (Table I). The band shift assay shown in Figure 2 demonstrated the presence of a cytoplasmic factor(s) in the IHF$^+$ strain and lacking from the IHF$^-$ counterpart which strongly bound to Pu. This protein–DNA complex was completely independent of the presence of XylR in the extracts and resisted displacement by a >1000-fold greater concentration of competitor DNA. To further confirm the identity of such a factor with IHF, we repeated the Pu band shift experiment with purified IHF protein introducing also as controls DNA restriction fragments carrying Pm (the promoter of the TOL *meta* cleavage pathway operon) and Ps (the promoter of the *xylS* gene). Figure 3 shows that at a concentration as low as 1 μg/ml of IHF, more than 70% of Pu was bound to IHF, suggesting an affinity constant in the range of that observed in the p'R promoter of lambda phage (Kur *et al.*, 1989). Under the same conditions, Pm showed no affinity at all for IHF whereas Ps showed some weak binding at high IHF concentrations (Figure 3). The effect of IHF on Ps activity was not further investigated. The precise DNA sequence within Pu which binds IHF was determined by DNase I footprinting (see below).

Hyperproduction of XylR and XylRΔC decreases Pu activity

To determine whether intracellular XylR concentration limits Pu expression, as it is the case for Pm and the XylS regulator (Mermod *et al.*, 1987), we carried out an induction experiment with *recA* strain BS288 which harbours a chromosomal *Pu–lacZ* fusion and a single copy *xylR* gene transformed with plasmid pEZ19, which carries *xylR* under the control of P*tac/lacI*^{q}. Results shown in Figure 4 demonstrate that (i) in the absence of upper pathway effectors like *p*-ClBA, XylR hyperproduction does not activate Pu, and (ii) in the presence of *p*-ClBA, hyperproduction of XylR led to a substantial decrease in the expression of the chromosomal fusion. A similar induction experiment in which a truncated derivative of XylR devoid of the potential DNA-binding domain (Inouye *et al.*, 1988) and Pu-activating activity named XylRΔC, was overproduced, is also shown in Figure 4. In this case, an approximately 50% decrease of *Pu–lacZ* activity was observed in respect to the control without XylRΔC. These experiments can be interpreted as if overproduction of both XylR and XylRΔC titers out a cellular factor(s) which is required for full Pu activity and probably interacts with a central domain of XylR protein (see Discussion).

Pu promoter region has potential to adapt bent structures

The bending of DNA regions upstream of positively-controlled promoters is being increasingly recognized as the critical event in triggering transcription initiation in both

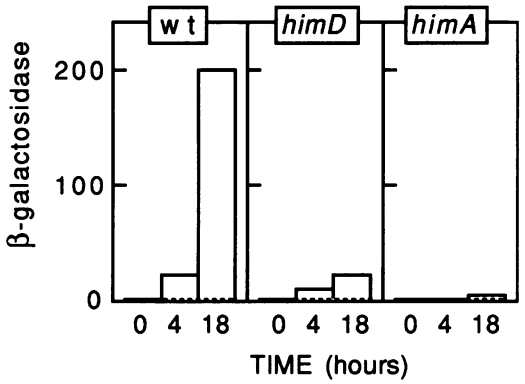

Fig. 1. Effect of IHF minus mutations on expression from the Pu promoter. *E.coli* strains BS294 (wt), BS297 (*himD*) and BS298 (*himA*) carrying chromosomal *Pu–lacZ* and *xylR* were grown in minimal M9 medium (Miller, 1972) with 0.1% casamino acids (M9CA) until late exponential phase (OD_{600} 1.2) after which were added with 2.5 mM *p*-ClBA (t = 0). Empty bars show the β-galactosidase levels [Miller units, (Miller, 1972)] of the corresponding cultures at the times indicated after inducer addition. Dashed bars indicate β-gal units of uninduced controls, which in most cases were below detection levels. *p*-ClBA addition did not significantly affect cell growth. β-galactosidase levels shown are the mean value of two independent measurements.

eukaryotic and prokaryotic systems (reviewed in Travers, 1990). Bracco *et al.* (1989) have demonstrated that native DNA curvatures may activate transcription even in the absence of the cognate binding proteins. To obtain a more complete picture of factors which may participate in Pu regulation, we subjected the Pu sequence (nucleotides −9 to −208 upstream of the transcription start) to an analysis of potential bent regions using Trifonov's criteria (Trifonov, 1985). Figure 5 shows the result of such an analysis. At least three regions within the sequence of interest have the potential to form bent structures. Relatively sharp bends occur in the left portion of the sequence, which coincide precisely with the regions of XylR interaction (see below).

XylR binds in vitro to at least two sites within the −121 to −178 bp upstream region of the Pu promoter and forms a complex 3-D structure

To localize the sites of interaction of the XylR protein within the Pu promoter region, we carried out DNase I footprinting experiments using as the source of Pu a 196 bp *Sma*I–*Alu*I restriction fragment spanning the region from the −12/−24 sequence of the σ^{54}(NtrA)-dependent promoter to −205 bp upstream of the transcription initiation site (Inouye *et al.*, 1984). This fragment contains all signals required to initiate XylR-mediated activation of Pu transcription (Inouye *et al.*, 1984; Dixon, 1986; Harayama *et al.*, 1989) and must therefore contain XylR-specific target sequences. As the source of XylR, we used an enriched fraction of a protein extract derived from a XylR-hyperproducing *E.coli* strain (Figure 6). To ensure that the interactions observed were due to XylR and not to other DNA-binding factors present in the protein fraction used, we systematically employed as a control an isogenic XylR$^-$ extract. Figure 7a shows the DNase I nicking patterns of the Pu-containing restriction fragment described before, labelled at the 3'-end of the lower band, in the presence of different concentrations of protein extract and *p*-ClBA. Figure 7b and c show a short and a long run, respectively, of the same experiment but using

Table I. Bacteria, phage and plasmids

E.coli K12 strain	Relevant genotype/characteristics	Reference/origin
CC118	Δ(*ara-leu*), *araD*, Δ*lacX* 74, *galE*, *galK*, *phoA*, *thi*-1, *rpsE*, *rpoB*, *argE* (Am), *recA*1	Herrero *et al.* (1990)
DPB101	Δ(*lac,pro*) *rpsL*, *himD451*::mini-*tet*	Biek and Cohen (1989)
DPB102	Δ(*lac,pro*) *rpsL*, *himA452*::mini-*tet*	Biek and Cohen (1989)
S90C	Δ(*lac,pro*) *rpsL*	Biek and Cohen (1989)
BS288	CC118 with chromosomal insertions mini-Tn*5* Sm/Sp *Pu*−*lacZ* and mini-Tn*10* Ptt *xylR/xylS*	This work
BS293	S90C with chromosomal insertion mini-Tn*5* Sm/Sp *Pu*−*lacZ*	This work
BS294	SC90 with chromosomal insertions mini-Tn*5* Sm/Sp *Pu*−*lacZ* and mini-Tn*10* Ptt *xylR/xylS*	This work
BS295	DPB101 with chromosomal insertion mini-Tn*5* Sm/Sp*Pu*−*lacZ* transduced from BS294	This work
BS296	DPB102 with chromosomal insertion mini-Tn*5* Sm/Sp *Pu*−*lacZ* transduced from BS294	This work
BS297	DPB101 with chromosomal insertions mini-Tn*5* Sm/Sp *Pu*−*lacZ* and mini-Tn*10* Ptt *xylR/xylS*	This work
BS298	DPB102 with chromosomal insertions mini-Tn*5* Sm/Sp *Pu*−*lacZ* and mini-Tn*10* Ptt *xylR/xylS*	This work

Plasmids	Genotype/Phenotype/Characteristics	Reference
pUJ9	Ap^r; promoter probe vector, *lacZ* fusion flanked by *Not*I sites	de Lorenzo *et al.* (1990)
pUJ11	Ap^r; pUJ9 with 298 bp *Sma*I−*Hae*III fragment of pED3306 inserted at *Sma*I site. *Pu*−*lacZ* fusion flanked by *Not*I sites.	This work
pUT/*Pu*−*lacZ*	Ap^r; pUT/mini-Tn*5* Sm/Sp with a *Pu*−*lacZ* insert from pUJ11 at *Not*I site	This work
pLysS	Cm^r; pACYC184 with T7 phage *lysS* gene cloned at *Bam*HI site	W.Studier
pPL401	Ap^r; pBR322 derivative containing Pm promoter of TOL in a *Sau*3A−*Bam*HI insert	Mermod *et al.*, 1984
pED3306	Ap^r; pBR322 derivative containing Pu promoter of TOL within a *Hin*dIII insert	Mermod *et al.* 1986
pKT570	Sm^r; pKT231 with a *xylR-xylS* insert as a 6 kb *Xho*I fragment	Mermod *et al.* 1986
pABOR7/*xylR-S*	Ap^r; pLOF/mini-Tn10 *Ptt* with a 6 kb *Not*I insert containing *xylR-xylS*	B.Kessler
pTrc99A	Ap^r; P*tac/lacI*^{q}-based expression vector. pBR322 replicon. *Nco*I site overlapping first structural ATG	Amann *et al.*, 1988
pVLT18	pMLB1034 (Silhavy *et al.*, 1984) inserted with a blunt-ended, Pm-containing 156 bp *Pst*I−*Taq*I fragment from pPL401 cloned at the *Sma*I site of the MCS. *Pm-lacZ* fusion plasmid	This work
pVLT47	Ap^r; pUC18 with a 196 bp *Sma*I−*Alu*I insert from pEZ9 containing Pu, cloned at *Sma*I site. Pu points towards *Hin*dIII site of pUC18 MCS	This work
pVLT48	Ap^r; pUC18 with a 196 bp *Sma*I−*Alu*I insert from pEZ9 containing Pu, cloned at *Sma*I site. Pu points towards *Eco*RI site of pUC18 MCS	This work
pMMB66EH	Ap^r; P*tac/lacI*^{q}-based expression vector. RSF1010 replicon	Furste *et al.* (1986)
pAZe3ss	Ap^r; P_L-based expression vector, *Nco*I−*Bam*HI−*Hin*dIII MCS, TIR of Mu *ner* gene, dowstream stop codons in all frames	Zaballos *et al.* (1987)
pEZ2a	Ap^r; pUC18 containing a 283 bp *Stu*I−*Taq*I fragment with the Ps-Pr divergent promoters of *xylS-xylR* from pKT570. Pr promoter points towards the *Eco*RI site of pUC18 MCS	This work
pEZ6	Ap^r; pTrc99A with an inserted 1.9 kb *Bam*HI/partial *Nco*I fragment. P*tac/lacI*^{q}-driven XylR overproduction	This work
pEZ9	Ap^r; pUC18 with the Pu-containing 312 bp *Eco*RI−*Bam*HI insert from pUJ11	This work
pEZ18	Ap^r; pMMB66EH inserted with 1.6 kb *Eco*RI−*Hin*dIII fragment encoding a COOH-truncated *xylR* sequence. P*tac/lacI*^{q}-driven XylRΔC overproduction	This work
pEZ19	Ap^r; pMMB66EH inserted with 1.9 kb *Bam* HI/partial *Nco*I fragment. P*tac/lacI*^{q}-driven XylR overproduction	This work

instead the 3′-end labelled upper band of the same restriction fragment as the source of Pu sequence.

Examination of the footprinting patterns of Figure 7a, b and c indicates that XylR binding involves primarily the region between −121 and −178 and results not only in stretches of protected bases, but also in several groups of hypersensitive sugar−phosphate bonds. This is currently explained by the induction of DNA bends which facilitate the DNase I nicking of the most exposed bases (Hochschild and Ptashne, 1986). Since such a phenomenon appears at least in three positions within the sequence affected, and all interactions seem to occur simultaneously regardless of protein concentration used, we conclude that XylR binding is cooperative and leads to a major change of the 3-D structure of the Pu upstream region. Nicking patterns of the control lanes from isogenic XylR$^-$ extracts (lanes 14 and 15 of Figure 7a, b and c) were not significantly different from those without any protein (lanes 1 and 2 of the same figure) confirming that the changes observed were due to XylR protein binding. Apart from the main region affected by XylR, we also observed some individual phosphodiester bonds to be hypersensitive to DNase I after XylR binding (for instance, see upper portion of Figure 7a). As these cannot represent alone XylR sites of binding, we attribute their existence to XylR-mediated indirect changes in accessibility to DNase I.

The summary of these interactions is depicted in Figure 8. There were similar protection patterns associated with the

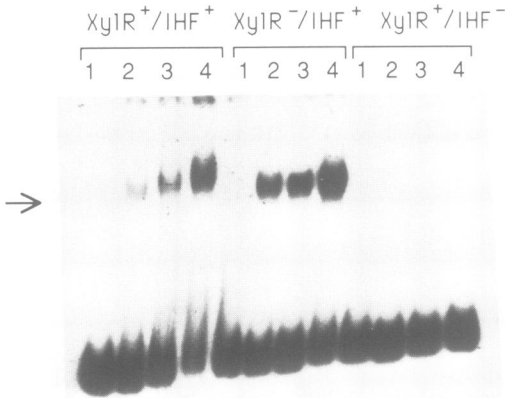

Fig. 2. Presence in *E.coli* cell extracts of a factor which binds strongly to the Pu promoter region. A radioactively labelled, Pu-containing 312 bp *Eco*RI−*Bam*HI fragment of pEZ9 (Table I) was diluted to ~0.1 nM in a buffer 20 mM Tris−borate pH 8, 50 μg/ml BSA, 0.1% Nonidet NP40, 40 mM KCl, 10% glycerol, 5 mM EDTA, 2 mM *p*-ClBA, 300 μg/ml of sonicated salmon sperm DNA and mixed with increasing amounts of protein extracts from strains XylR$^+$/IHF$^+$ (*E.coli* CC118 /pEZ6,pLysS), XylR$^-$/IHF$^+$ (*E.coli* CC118/pTrc99A,pLysS) and XylR$^+$/IHF$^-$ (*E.coli* DPB102/pEZ6,pLysS) as indicated at the top of the figure. Amounts of protein extracts added in a final volume of 20 μl were: lanes 1, none; lanes 2, 2 μg; lanes 3, 3 μg; lanes 4, 10 μg. After preincubating 10 min at 30°C, samples were loaded on a gel (4% acrylamide, 20 mM Tris−borate pH 8, 2 mM *p*-ClBA, 5 mM EDTA) and run with the same gel buffer at 10 V/cm for 5 h. The gel was subsequently autoradiographed.

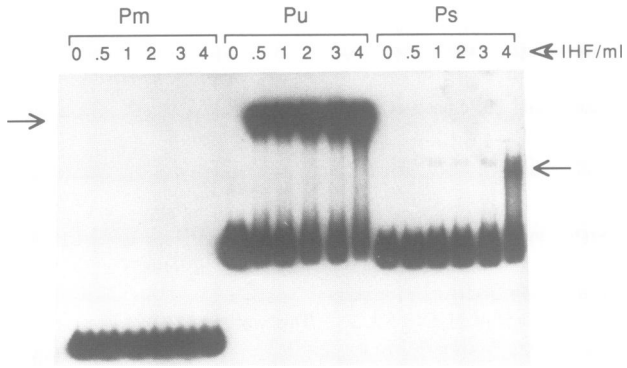

Fig. 3. IHF binding assays to Pm, Pu and Ps promoters of TOL plasmid. End-labelled restriction fragments containing the sequences of the TOL promoters (see text) indicated at the top of the figure were diluted to ~ 0.1 nM in a buffer 25 mM Tris−HCl pH 7.5, 50 mM KCl, 10% glycerol, 1 mM EDTA, 2 mM $MgCl_2$, 1 mM Ca^{2+}, 100 μg/ml BSA and 5 μg/ml competitor DNA and mixed with increasing amounts of purified IHF (concentrations are given in μg/ml) in a final vol of 20 μl as indicated. After 30 min preincubation at 30°C, samples were loaded onto a gel (4% acrylamide, 25 mM Tris−HCl pH 7.5, 1 mM EDTA) and run for 4 h at 8 V/cm in the same gel buffer. Arrows indicate the position of the strong complex with Pu (arrow on left) and the weak complex with Ps (arrow on right).

homologous sequences designated b (5′-TTGAT-3′) and c (5′-CAAATC-3′) but also near identical protection patterns observed with sequences which share little or no homology (those designated a and hinge). As shown in Figure 8, the joint a-b-c group of interactions appears twice in inverted orientation (a-b-c: −178 to −162 and c-b-a: −137 to −121) whereas one additional a-b group (−148 to −138) appears

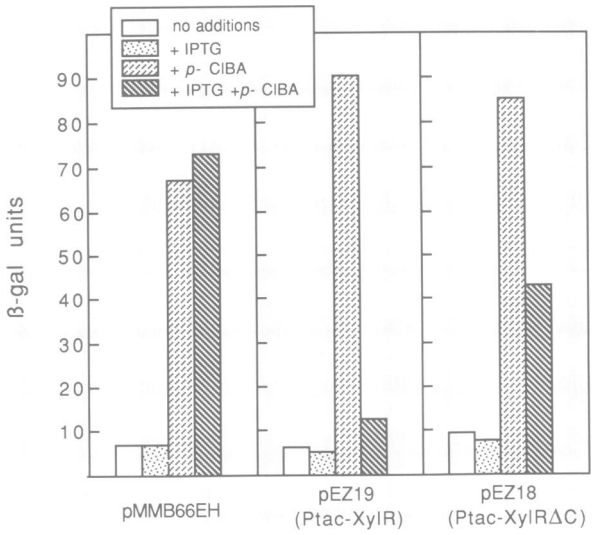

Fig. 4. Effect of XylR and XylRΔC hyperproduction on expression from the Pu promoter. Strain *E.coli* BS288 containing chromosomal insertions with *Pu−lacZ* and *xylR* was transformed with plasmids pMMB66EH (control), pEZ19 (P*tac/lacI^q*-driven *xylR* expression) and pEZ18 (P*tac/lacI^q*-driven *xylR* ΔC expression) as indicated at the bottom of the figure. Strains were grown at 30°C in M9CA medium to an OD_{600} of 0.4, after which point 150 μM IPTG, 2 mM *p*-ClBA or 150 μM IPTG+2 mM *p*-ClBA were added. Growth was not significantly affected by the additions. The figure shows the mean value of three independent measurements of the β-galactosidase levels (Miller, 1972) of the cultures after a 16 h induction period.

contiguous with the c-a-b sequence. We have given the names UBS1 (UBS: upstream binding sequences) and UBS2 to the further upstream group of interactions abc and to the whole ab/cba group, respectively. The hinge region in between the two UBSs has little sequence homology to other groups of bases in the region and we therefore believe that the corresponding protected/hypersensitive bases are the result of a local change in the DNA conformation rather than a direct interaction with XylR. Figure 7 shows also that in the conditions used here, addition of *p*-ClBA had no detectable influence on XylR binding in the range of concentrations used. It should be noted, however, that XylR$^+$ extracts were obtained from cells grown in the presence of *p*-ClBAd (see Materials and methods) and therefore XylR might be pre-activated.

Identification of the IHF binding site

The same DNase I footprinting procedure was used to localize the site of IHF interaction with Pu. Figure 7a and b show that IHF protection spans the region between −52 to −79, which contains an IHF-consensus site 5′-WATCAANNNNTTR-3′ (Friedman, 1988; Yang and Nash, 1989). As mentioned below, addition of a higher IHF concentration did not extend the protection pattern, thus confirming that only one site was present in the region.

Independent IHF and XylR binding to Pu

Since both IHF and XylR bind to the Pu upstream sequence *in vitro* and participate in promoter activation *in vivo* (see above), it was interesting to ascertain whether IHF facilitates XylR binding to UBS1 and UBS2 or vice versa. In the experiment shown in Figure 9, different amounts of XylR-containing extract were added to binding mixtures pre-incubated with varying amounts of IHF. The resulting DNase

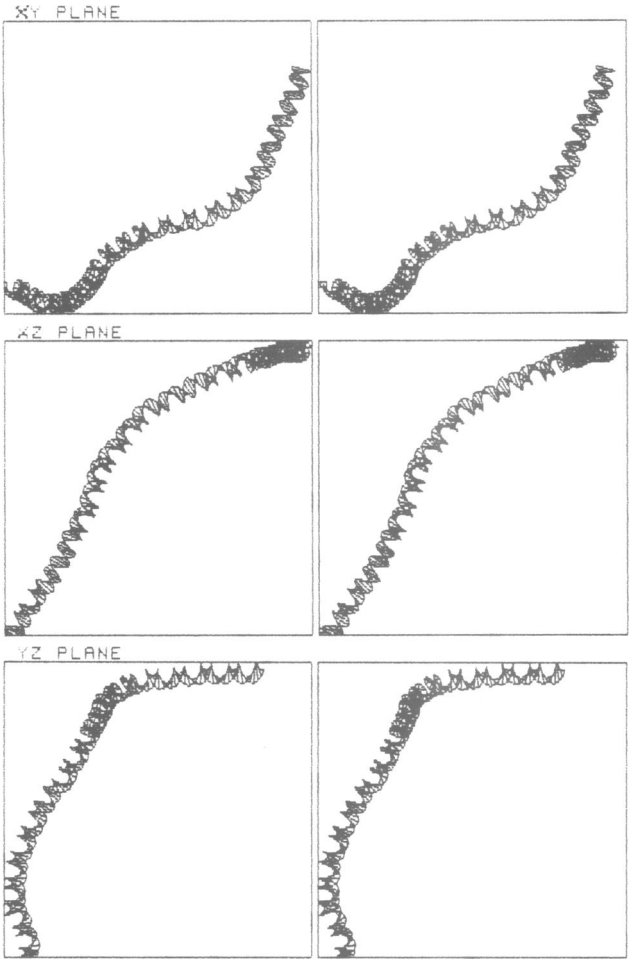

Figure 5. Three-dimensional distribution of bends in the DNA structure of the Pu sequence. A bending analysis of the Pu promoter region (nucleotides −208 to −9 from transcription initiation site) was carried out as indicated in Materials and methods. Stereoscopic projections of the predicted shapes from three different planes are shown. The left of the XY and XZ planes corresponds to the 5′-end of the −208 extremities.

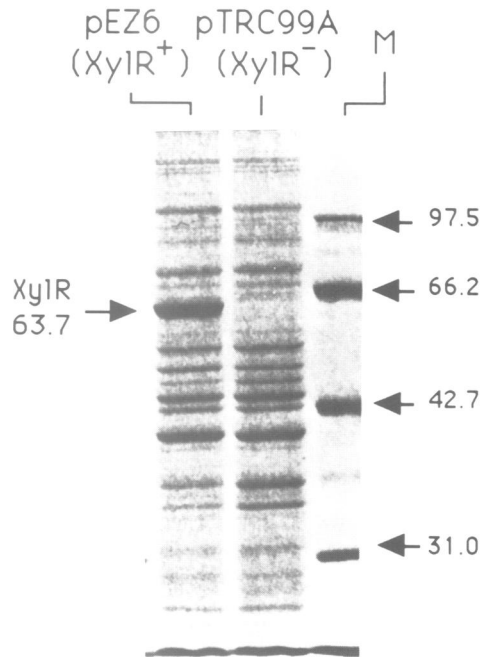

Figure 6. SDS−PAGE analysis of XylR$^+$ and XylR$^-$ protein extracts used in footprinting experiments. 4 μg of protein extracts derived from *xylR*$^+$ strain *E.coli* CC118(pEZ6.pLysS) and *xylR*$^-$ control *E.coli* CC118(pTrc99A.pLysS) were run on a 8% SDS−PAGE gel and stained with Coomassie blue. Size standards are indicated in kilodaltons.

I-nicking pattern showed that XylR-induced changes and IHF binding to Pu are completely independent.

Discussion

The activity of the Pu promoter of the operon specifying transformation of toluene/xylenes to aromatic carboxylic acids is controlled by several regulatory proteins which translate the presence of substrates of the upper TOL operon into activation of transcription of the corresponding catabolic genes. In this paper we examine the *in vitro* interactions of two such regulators, XylR and IHF with sequences located upstream of the transcription initiation site and from our findings develop a mechanistic model to account for the effects observed *in vivo*.

The presence of an IHF-binding consensus sequence within Pu and homologous sequences in other σ^{54}-dependent promoters (Holtel *et al.*, 1990; Hoover *et al.*, 1990; Gober and Shapiro, 1990) led us to investigate its effect *in vivo*. Results shown in Figure 1 indicate that IHF indeed influences Pu expression. Since we had previously had inconsistent results using multicopy plasmids care was taken to carry out the β-galactosidase assays for the *xylR/Pu−lacZ* system in single copy dosage (see Materials and methods). In *E.coli*, IHF is required for many cell functions, including expression of several bacterial and phage genes (Kur *et al.*, 1989; Pereira *et al.*, 1988; Krause and Higgins, 1986; reviewed in Friedman, 1988). The sign of IHF effect seems to depend on the phasing and orientation of the IHF-induced DNA bend in respect to the transcription initiation site or the recombination complex (Huang *et al.*. 1990; Thompson and Mossig, 1988; Goodman and Nash, 1989; Snyder *et al.*, 1989). σ^{54}(NtrA)-dependent promoters seem to share the need for specific activator proteins and cognate upstream sequences (UAS) for productive transcription initiation through a mechanism that involves DNA looping : If IHF-induced bends bring activator−UAS complexes into close proximity with bound RNA polymerase, IHF may facilitate transcription initiation (Kustu *et al.*, 1989; Hoover *et al.*, 1990; Ninfa *et al.*, 1987; Gober and Shapiro, 1990).

The cylindrical projection of the helix sides on Pu sequence (not shown) indicates that if the middle of the IHF-binding consensus sequence present in Pu is considered to be the centre of the DNA bend, then the side of the helix which contains the −12 and −24 elements of the Pu promoter (Dixon, 1986) is virtually opposite to that contacted and bent by IHF (Figure 10). The orientation of the IHF- and XylR-induced bends (see below) is such that if the −12 and −24 elements are located on the top of the helix (and therefore σ^{54}−RNA polymerase also contacts the top of the helix) as depicted in Figure 10, then bending at the IHF site brings the upstream XylR/UBSs into contact with the underside or one flank of the bound σ^{54}-RNA polymerase, resulting in the formation of a productive transcription initiation complex. Whether or not the same applies to other σ^{54}-dependent instances (Hoover *et al.*, 1990; Gober and

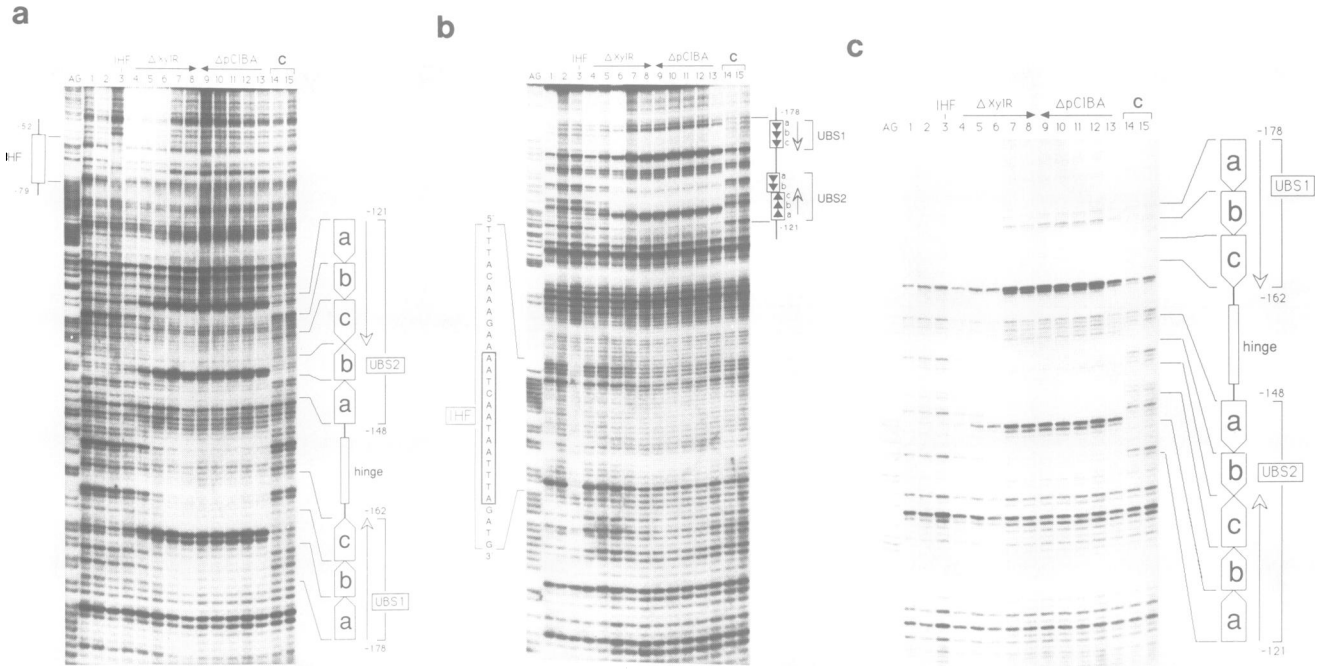

Fig. 7. XylR/IHF interactions with Pu upstream sequences. **a** is a short run of a footprinting experiment carried out on the 221 bp *Eco*RI−*Bam*HI fragment of pVLT47 labelled in 3′ at the *Eco*RI end (label on the lower band of Pu sequence in Figure 8), whereas **b** and **c** show short and long runs respectively of the same experiment carried out with the equivalent fragment from pVLT48 (label on 3′ end of upper band of Pu sequence). Each end-labelled restriction fragment was subjected to DNase I nicking in the presence of different amounts of $XylR^+$ and $XylR^-$ protein extracts as follows: lane 1, no additions; lane 2, 3 mM *p*-ClBA; lane 3, 3 mM *p*-ClBA plus 3 μg/ml pure IHF; lane 4, 3 mM *p*-ClBA plus 1 μg $XylR^+$ extract; lane 5, 3 mM *p*-ClBA plus 2 μg $XylR^+$ extract; lane 6, 3 mM *p*-ClBA plus 6 μg $XylR^+$ extract; lane 7, 3 mM *p*-ClBA plus 12 μg $XylR^+$ extract; lane 8, 3 mM *p*-ClBA plus 20 μg $XylR^+$ extract; lane 9, 2 mM *p*-ClBA plus 20 μg $XylR^+$ extract; lane 10, 1 mM *p*-ClBA plus 20 μg $XylR^+$ extract; lane 11, 0.3 mM *p*-ClBA plus 20 μg $XylR^+$ extract; lane 12, 0.1 mM *p*-ClBA plus 20 μg $XylR^+$ extract; lane 13; 20 μg $XylR^+$ extract, no inducer; lane 14, 3 mM *p*-ClBA plus 20 μg $XylR^-$ extract; lane 15, 20 μg $XylR^-$ extract, no inducer. AG lane coresponds to the A+G Maxam and Gilbert sequencing reaction. Arrows on top of the figure summarize the different additions to the samples, as well as the increasing or decreasing amounts of protein extract and Pu inducer, *p*-ClBA. The C on top of lanes 14 and 15 points out the control lanes with the samples from the $XylR^-$ extracts. Lateral drawings locate the major zones of DNA−protein interaction (see text).

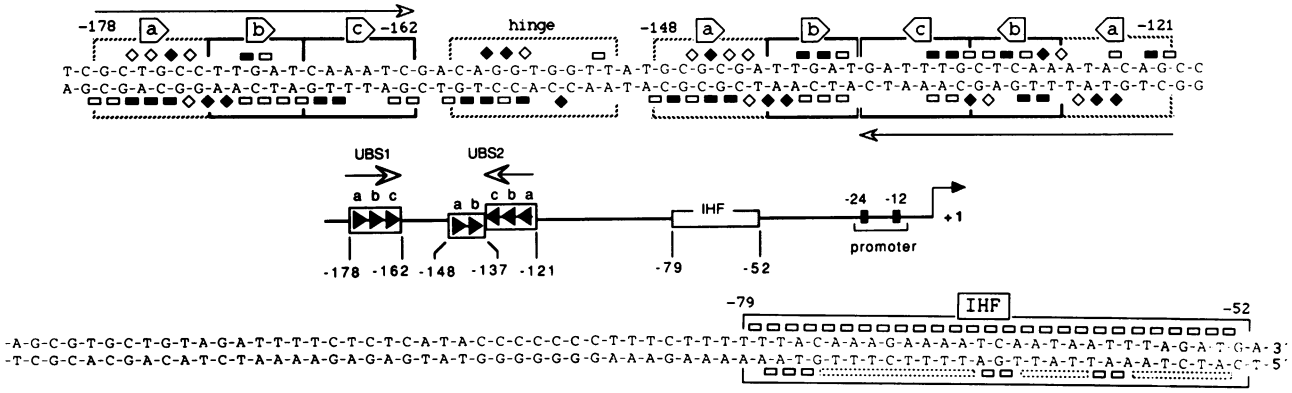

Fig. 8. Summary of XylR/IHF interactions in the Pu sequence. DNA sequences represented on top and bottom of the figure span the Pu region between −180 to −51 (Inouye *et al.*, 1984), where all major interactions are localized. Solid and hollow symbols on top of nucleotides indicate respectively the location of strong and weak protected (boxes) or hypersensitive (diamonds) sugar−phosphate bonds. Only groups of interactions and bases affected by $XylR^+$ extracts but not by $XylR^-$ have been considered. Solid lines indicate homologous sequences within the zone of interactions whereas dashed lines indicate sequences altered upon XylR binding which share little or no homology with one another or with the homologous sequences. Sequences affected by XylR were operatively placed in two groups, denominated upstream binding sequence 1 and 2 (UBS1 and UBS2). The long dashed boxes on the bottom of the lower band of the IHF-binding sequence represent groups of bases which appeared to be affected as a whole by IHF in Figure 7a but in which we could not differentiate the effect on individual bonds. A summary of the interactions is given in the middle of the figure along with the IHF-binding region and the −12/−24 sequences of the Pu promoter.

Shapiro, 1990) does deserve further investigation, although we have already observed that in the analogous system NifA/P*nifH*, the −12/−24 promoter elements and the center of the potential IHF-bent sequence (Santero *et al.*, 1989; Hoover *et al.*, 1990) are located also on virtually opposite DNA helix sides.

Since our efforts to obtain purified XylR have failed so far due to the tendency of the protein to form insoluble aggregates, XylR binding to Pu was investigated in DNase I footprinting experiments using a XylR-enriched protein fraction obtained from hyperproducing *E.coli* cells., along with a control isogenic $XylR^-$ extract. The DNase I

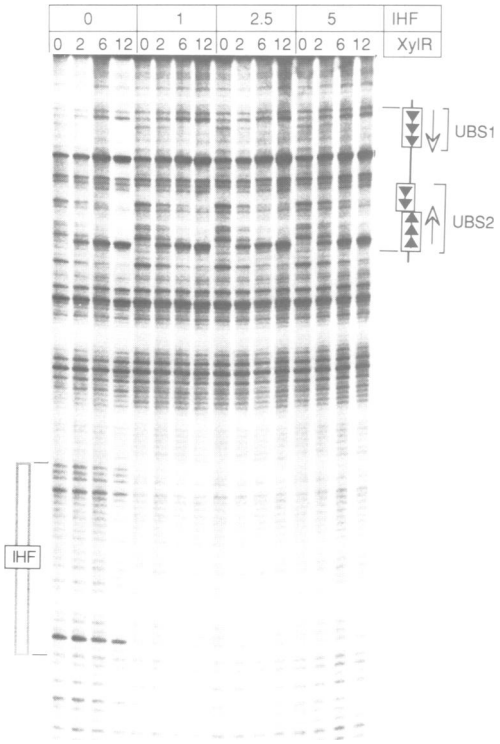

Fig. 9. Simultaneous XylR/IHF binding to different Pu locations. The autoradiograph shows the result of a competition experiment between XylR and IHF carried out on a restriction fragment derived from pVLT48 (labelled at the 3′-end of upper band, Figure 8). Footprinting reactions were set up as usual in a final vol of 100 μl, but labelled fragments were preincubated for 5 min with the amounts (in μg/ml) of IHF indicated on top of the figure before addition of increasing amounts of $XylR^+$ extract (indicated in μg on the gel heading). Lateral drawings show the position of UBS elements and the IHF binding site as discussed in the text. Note little or no mutual influence of XylR binding on IHF and vice versa, although a minor hypersensitivity of about 12 bp in between their respective binding sites becomes apparent

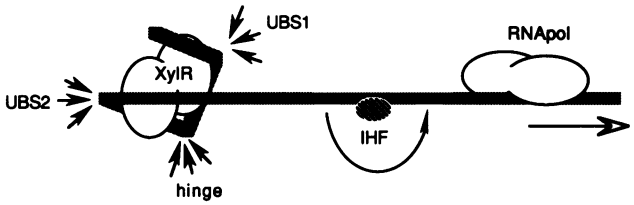

Fig. 10. Simplified model of Pu activation by XylR and IHF. This depiction of the possible distribution of elements controlling Pu expression is based on the DNase I footprinting experiments of Figure 7 and the location of the observed interactions on the surface of a cylindrical projection of the Pu sequence. DNA hypersensitive spots starting at about −121 (Figure 8) are considered the vertex of relatively sharp bends leading to the formation of a triangular pocket which may accomodate two XylR units or DNA binding domains. Specific interactions would take place through sequences designated bc (5′-TTGANCAAATC-3′) contained in inverted orientation in UBS1 and UBS2 (see Figure 8), whereas the rest of the changes would be the result of an altered DNA structure. Arrows indicate the approximate locations of the DNase I-hypersensitive patches. The region named hinge in the figure includes not only the sequence designated hinge in Figure 8, but also a portion of the nearby 'a' sequence, the hypersensitive portions of which happen to be on the same DNA helix side. Orientation of the IHF-induced bend is also indicated as well as the position of the σ^{54}-RNA polymerase binding at sequences −12/−24. Protein sizes are symbolic.

protection patterns obtained (Figure 7) were very complex, being interpreted as the result of major conformational changes in the upstream region upon activator binding. XylR-induced changes along with those produced by IHF probably result in the formation of a higher order nucleoprotein structure -yet simpler than those proposed for the *malEp-malKp* (Raibaud *et al.*, 1989) or the *pflaN-pflbG* promoters (Gober and Shapiro, 1990). In only two of the protected sequences, those named b (5′-TTGAT-3′) and c (5′-CAAATC-3′), there is a correlation between the observed pattern of interactions and sequence homology. It is therefore likely that the actual sequence recognized by XylR includes a motif 5′-TTGANCAAATC-3′. This sequence appears twice, in inverted orientation, within the groups of interactions that we have named UBS1 and UBS2 and is contained within the consensus sequence proposed by Holtel *et al.* (1990). It also overlaps with two of the three Pu upstream regulatory sequences (URS3 and URS1) identified by Inouye *et al.* (1990) by deletion analysis.

To obtain an impression of the three-dimensional distribution of XylR interactions, we made computer modelling using a commercial program (see Materials and methods). Placing the hypersensitive bonds (diamonds in Figure 8) on a cylindrical projection of the Pu sequence reveals that they cluster in three patches on different helix sides. The first patch is formed by bonds included mostly in sequence a of UBS1. This is separated from the second patch by one protected helix turn. The second group contains hypersensitive bonds present in the hinge region and the a sequence of the ab portion of UBS2, including therefore bonds on the same side of two helix turns. One more protected helix turn separates this group from the third hypersensitive patch, which coincides with the promoter-proximal a sequence of UBS2 of Figure 8 (not shown). By bending the DNA cylinder at the three patches of hypersensitivity, a triangular pocket is obtained which could probably wrap around two XylR monomers or at least two DNA-binding domains of XylR. Figure 10 summarizes these interactions and suggests a plausible model to account for the features described. In this model, XylR and IHF binding are independent and, as mentioned above, activation of transcription is achieved by bringing XylR/UBS as a whole into close proximity to a lower or a lateral zone of the σ^{54}−RNA polymerase complex. The three-dimensional model of Figure 10 is indeed an oversimplification, since in addition to XylR and IHF-induced bends, the Pu sequence also has the potential to form native, non-linear structures (Figure 5). Other σ^{54}-dependent activators like NtrC do not seem to generate such drastic bending of the cognate DNA sequences, at least as far as can be detected by DNase I footprinting (Hirschman *et al.*, 1985; Ninfa *et al.*, 1987).

Unlike other σ^{54}-dependent activators such as NifA proteins from *Klebsiella pneumoniae* (Buck and Cannon, 1989; Morett *et al.*, 1988) and *Rhizobium meliloti* (Huala and Ausubel, 1989), XylR requires for activity the presence of the COOH terminal domain of the protein thought to be involved in DNA recognition (data not shown). Furthermore, *in vivo* competition experiments of Figure 4 indicate that overproduction of either XylR or its truncated derivative devoid of such a domain lead to a significant inhibition of Pu activity. A plausible explanation for this effect could be that XylR interacts with at least one other regulatory factor that is titrated by excess of acceptor protein. If this is the case, inhibition of Pu by overproduced XylR would be

mechanistically similar to the squelching of eukaryotic promoters (Ptashne, 1988; Levine and Manley, 1989).

Materials and methods

Strains, transposons, plasmids and media

The relevant properties of the strains and constructions used in this work are listed in Table I. Isogenic *E.coli himA*$^+$*himD*$^+$ (IHF$^+$), *himA*$^-$*himD*$^+$ (IHF$^-$) and *himA*$^+$*himD*$^-$ (IHF$^-$) strains containing the *xylR* gene and a *Pu*−*lacZ* fusions integrated into the chromosome were constructed as follows. A specialized mini-Tn*5* transposon containing a *Pu*−*lacZ* fusion was generated by cloning a Pu-containing 298 bp *Sma*I-*Hae*III fragment of the TOL plasmid (Inouye *et al.*, 1984; Dixon, 1986) into the single *Sma*I site of pUJ9 vector (de Lorenzo *et al.*, 1990) to produce pUJ11. The 4.2 kb *Not*I fragment containing the *Pu*−*lacZ* fusion was then cloned into the single *Not* I site of the mini-Tn*5Sm/Sp* element (de Lorenzo *et al.*, 1990) in the orientation which results in the presence of an interposon (i.e., a strong transcriptional terminator Ω element, Prentki and Krisch, 1984) upstream of the Pu promoter. The resulting hybrid transposon was then inserted into the chromosome of *E.coli* S90C strain (*himA*$^+$*himD*$^+$) with selection for spectinomycin resistance as described earlier (de Lorenzo *et al.*, 1990), to produce strain BS293. The *xylR* gene was subsequently transposed to the chromosome of BS293: an ~6 kb *Xho*I fragment of pKT570 (Mermod *et al.*, 1986), was added with *Not*I ends and subcloned into the *Not*I site of a bialaphos resistance mini-Tn*10* element (Herrero *et al.*, 1990; B.Kessler, V.de Lorenzo and K.N.Timmis, in preparation) to produce BS294 (Table I). This *Pu*−*lacZ/xylR*$^+$ strain was then used to grow P1*vir* phage in order to transduce the now chromosomal *Pu*−*lacZ* insert into the IHF$^-$ isogenic strains DPB101 and DPB102 (producing, BS295 and BS296 respectively). A second round of transposition was employed to additionally insert the *xylR* -containing fragment, to produce BS297 and BS298. The same strategy was followed to introduce *Pu*−*lacZ* and *xylR* monocopy insertions into *E.coli* CC118 strain to produce BS288 (*E.coli* CC118 *Pu*−*lacZ/xylR*$^+$).

Construction of XylR and XylRΔC-overproducing E.coli strains

An *Nco*I site overlapping the first ATG of the *xylR* structural gene was generated by site-directed mutagenesis (Kunkel *et al.*, 1987) and the resulting construct was then added with a dowstream *Bam*HI site and finally inserted as a partial 1.9 kb *Nco*I−*Bam*HI fragment into the corresponding sites of vector pTrc99A (Amann *et al.*, 1988), which placed its expression under the regulated control of the P*tac* promoter and provided *xylR* with an improved translation initiation region (TIR). The base changes resulting from the introduction of the *Nco*I site led to a conservative Ser to Ala change at the second position of the protein sequence. The resulting plasmid (pEZ6) directed the overproduction of XylR protein in a variety of *E.coli* strains when induced with IPTG (isopropyl-β-D-thiogalactopyranoside). The protein was detectable as an ~64 kd band in SDS−PAGE protein gels and was active in DNA footprinting experiments (see Results).

For *in vivo* analysis of XylR and its COOH-terminal truncated derivative XylRΔC, two more plasmids directing hyperexpression of these proteins were constructed. pEZ19 provides the P*tac*/*lac*^{Iq}-driven transcription of *xylR* in the broad host range plasmid pMMB66EH (Furste *et al.*, 1986) and utilizes the TIR of the *ner* gene of Mu phage for an efficient translation (Zaballos *et al.*, 1987). pEZ18 provides a similar expression system for a truncated XylR derivative of an ~56 kd (named XylRΔC) specified by a gene in which a stop codon had been introduced immediately after the *Nco*I site located at the 1577 bp position of the *xylR* sequence (Inouye *et al.*, 1988) through the subcloning of the 1.5 kb *Nco*I fragment of pEZ6 into the pAZe3ss vector (Zaballos *et al.*, 1987). The new stop codon eliminates the last 39 amino acids of the protein, which are believed to participate in DNA binding (Inouye *et al.*, 1988).

Protein techniques

Preparation of XylR$^+$ and XylR$^-$ protein extracts was made as follows. The *E.coli* strains indicated in each case were transformed with pEZ6 (*xylR*$^+$) and pLysS, which encodes the *lysS* lysis gene of T7 phage (W.Studier, personal communication) and facilitates the preparation of protein extracts (see below). A *xylR*$^-$ isogenic strain was obtained by co-transforming competent cells with the pTrc99A vector along with pLysS. *xylR*$^+$ and *xylR*$^-$ *E.coli* strains were grown in liquid BHI medium (Difco) at 30°C with good aeration up to an OD_{600} of 0.5, at which point 0.25 mM IPTG and 1 mM *p*-chlorobenzylaldehide (*p*-ClBAd) were added; the incubation was continued overnight. Cells were then pelleted and resuspended in 1/10 to 1/20 of the initial culture vol of 20 mM Tris−HCl pH 8, 10% glycerol, 0.1% Triton X-100, 2 mM β-mercaptoethanol buffer, after which they were subjected to at least 3 cycles of freezing in liquid nitrogen and thawing at 30°C until LysS-mediated quantitative lysis of the cells was achieved. The lysates were then sonicated briefly to decrease their viscosity, spun down at low speed to remove cell debris and fractionated with ammonium sulfate (AS). Virtually all soluble XylR protein (detectable as a 64 kd protein band present in the *xylR*$^+$ extract and absent in the isogenic *xylR*$^-$) was within the 20-40% saturated AS fraction (see Results section). Prior to the *in vitro* assays described below, AS was removed from the protein extracts by overnight dialysis against 20 mM Tris−HCl pH 8, 15% glycerol, 5 mM β-mercaptoethanol, 2 mM EDTA buffer.

Gel retardation assays and footprinting experiments

Monitoring of strong Pu-binding activities was carried out by gel retardation, using conditions described in Results section. To separately end-label each strand of a 196 bp *Sma*I−*Alu* I restriction fragment from pED3306 (Mermod *et al.*, 1986) containing Pu, the restriction fragment was cloned in both orientations at the *Sma*I site of pUC18 yielding pVLT47 and pVLT48. The resulting 221bp *Eco*RI−*Bam* HI fragments (identical excepting for the orientation of the *Eco*RI−*Bam*HI ends) were then purified and incubated independently with AMV reverse transcriptase along with [α-^{32}P]dATP in the presence of dTTP as described (de Lorenzo *et al.*, 1988) and further chased for 10 min with a mixture of 2.5 mM cold dNTPs. Such a treatment incorporates ^{32}P exclusively at the *Eco*RI ends, and results in the separate radioactive labelling of each of the DNA strands of otherwise identical fragments. A similar procedure was used to end-label a longer (298 bp) *Sma*I−*Hae*III restriction fragment from pED3306 containing also Pu, as well as a 283 *Stu*I−*Taq*I fragment from pKT570 (Mermod *et al.*, 1986) containing the divergent Ps-Pr promoters (Inouye *et al.*, 1987) and a 156 bp *Pst*I−*Taq*I fragment of pPL401 (Mermod *et al.*, 1984) containing the Pm promoter sequence of the *meta* cleavage pathway operon.

DNase I footprints of purified IHF protein (a kind gift of Howard Nash), XylR$^+$ and XylR$^-$ protein extracts on Pu promoter were made as detailed previously (de Lorenzo *et al.*, 1988). For each DNase I-nicking reaction, end-labelled fragments containing Pu were diluted to ~0.5 nM in a final vol of 100 μl of a buffer consisting of 20 mM Tris−HCl pH 7.4, 2 mM $MgCl_2$, 1 mM $CaCl_2$, 0.1 mM EDTA, 40 mM KCl, 100 μg/ml BSA, 20 μg/ml competitor DNA and preincubated for 3 min at 30°C with various amounts of protein extract, after which 2.5 ng of DNase I (Fluka) was added and the incubation continued for 2 min. Reactions were then stopped by addition of 50 μl of STOP buffer containing 0.1 M EDTA pH 8, 0.8% SDS, 1.6 M NH_4Ac, 300 μg/ml sonicated salmon sperm DNA. Nucleic acids were then precipitated with 350 μl of ethanol, lyophilized and directly resuspended in 90% formamide (with tracking dyes) prior to loading on a 7% DNA sequencing gel. A+G Maxam and Gilbert reactions (Maxam and Gilbert, 1980) were carried out with the same fragments and loaded in the gels along with the footprinting samples.

DNA analysis

Cylindrical projection of DNA sequences and bending analysis were performed by the use of the DNASTAR computer programs (DNASTAR, Inc., UK). The A−A wedge angle was estimated to be 8.6° as calculated by Trifonov (1985).

Acknowledgements

Authors are indebted to E.Amann, T.Kholer, S.Harayama, Birgit Kessler, M.Buck, M.Bagdasarian, W.Studier, J.L.Ramos and H.Nash for the kind gift of plasmids and/or materials. A.Zulueta and J.Pérez Martin are also acknowledged for their help with DNA analysis computer programs and helpful discussions, as is Ute Jacubzik for superb technical assistance. During the period of time spanning this investigation, M.H. was a postoctoral BAP-EC grantee. The portion of this work carried out by V.D.L. in Madrid was funded by Grant BIO89-0497 of the Spanish Comisión Interministerial de Ciencia y Tecnología.

References

Abril,M.A., Michan,C., Timmis,K.N. and Ramos,J.L. (1989) *J. Bacteriol.*, **171**, 6782−6790.

Amann,E., Ochs,B. and Abel,K.J. (1988) *Gene*, **69**, 301−315.

Biek,D. and Cohen,S.N. (1989) *J. Bacteriol.*, **171**, 2056−2065.

Bracco,L., Kotlarz,D., Kolb,A., Diekmann,S. and Buc,H. (1989) *EMBO J.*, **8**, 4289−4296.

Buck,M. and Cannon,W. (1989) *Nucleic Acids Res.*, **17**, 2597−2612.

Buck,M., Cannon,W. and Woodcock,J. (1987) *Mol. Microbiol.*, **1**, 243–249.
Dixon,R. (1986) *Mol. Gen. Genet.*, **203**, 129–136.
Friedman,D.I. (1988) *Cell*, **55**, 545–554.
Furste,J.P., Pansegrau,W., Frank,R., Blöcker,H., Scholz,P., Bagdasarian,M. and Lanka,E. (1986) *Gene*, **48**, 119–131.
Gober,J. and Shapiro,L. (1990) *Genes Dev.*, **4**, 1494–1504.
Goodman,S. and Nash,H.A. (1989) *Nature*, **341**, 251–254.
Harayama,S. and Timmis,K.N. (1989) In Hoopwod,D and Chater,K. (eds) *Genetics of Bacterial Diversity.* Academic Press, London. pp. 151–174.
Harayama,S., Rekik,M., Wubbolts,M., Rose,K., Leppik. and Timmis,K.N. (1989) *J. Bacteriol.*, **171**, 5048–5055.
Herrero,M., de Lorenzo,V. and Timmis,K.N. (1990) *J. Bacteriol.*, **172**, 6557–6567.
Hirschman,J., Wong,K., Sei,K., Keener,J. and Kustu,S. (1985) *Proc. Natl. Acad. Sci. USA*, **82**, 7525–7529.
Hochschild,A.H. and Ptashne,M. (1986) *Cell*, **44**, 681–687.
Holtel,A., Abril,M.A., Marques,S., Timmis,K.N. and Ramos,J.L. (1990) *Mol. Microbiol.*, **4**, 1551–1556.
Hoover,T., Santero,E., Porter,S. and Kustu,S. (1990) *Cell*, **63**, 11–22.
Huang,L., Tsui,P. and Freundlich,M. (1990) *J. Bacteriol.*, **172**, 5293–5298.
Huala,E., and Ausubel,F. (1989) *J. Bacteriol.*, **171**, 3354–3365.
Inouye,S., Nakazawa, A and Nakazawa,T. (1984) *Proc. Natl. Acad Sci. USA.*, **81**, 1688–1691.
Inouye,S., Nakazawa,A. and Nakazawa,T. (1987) *Proc. Natl. Acad Sci. USA.*, **84**, 5182–5186.
Inouye,S., Nakazawa,A. and Nakazawa,T. (1988) *Gene*, **66**, 301–306.
Inouye,S., Yamada,M., Nakazawa,A. and Nakazawa,T. (1989) *Gene*, **85**, 145–152.
Inouye,S., Gomada,M., Sangodkar,U.M., Nakazawa,A. and Nakazawa,T. (1990). *J. Mol. Biol.*, **216**, 251–260.
Köhler,T., Harayama,S., Ramos,J.L. and Timmis,K.N. (1989) *J. Bacteriol.*, **171**, 4326–4333.
Krause,H.M. and Higgins,N.P. (1986) *J. Biol. Chem.*, **261**, 3744–3752.
Kunkel,T. A., Roberts,J.D. and Zakour,R.A. (1987) *Methods Enzymol.*, **154**, 367–382.
Kur,J., Hasan,N and Szybalski,W. (1989) *Gene*, **81**, 1–15.
Kustu,S., Santero,E., Keener,J., Popham,D. and Weiss,D. (1989) *Microbiol. Rev.*, **53**, 367–376.
Levine,M. and Manley,J. (1989) *Cell*, **59**, 405–408.
Lorenzo,V. de, Giovannini,F., Herrero,M and Neilands,J.B. (1988) *J. Mol. Biol.*, **203**, 875–884.
Lorenzo,V. de, Herrero,M. and Timmis, K.N. (1990) *J. Bacteriol.*, **172**, 6568–6572.
Maxam,A. and Gilbert,W. (1980) *Methods Enzymol.*, **65**, 499–560.
Mermod. N., Harayama,S. and Timmis,K.N. (1986) *Bio/Technology*, **4**, 321–324.
Mermod. N., Lehrbach,P.R., Reineke,W. and Timmis,K.N. (1984) *EMBO J.*, **3**, 2461–2466.
Mermod. N., Ramos,J.L., Bairoch,A. and Timmis,K.N. (1987) *Mol. Gen. Genet.*, **207**, 349–354.
Miller,J.H. (1972) *Experiments in Molecular Genetics.* Cold Spring Harbor Laboratory Press, Cold Spring Harbor, NY.
Morett,E., Cannon,W and Buck,M. (1988) *Nucleic Acids Res.*, **16**, 11469–11488.
Morett,E. and Buck,M. (1988) *Proc. Natl. Acad. Sci. USA*, **85**, 9401–9405.
Nakazawa,T, Inouye,S. and Nakazawa,A. (1990) In Silver,S., Chakrabarty,A., Glewski,I and Kaplan,S (eds) *Pseudomonas: Biotransformations, Pathogenesis and Evolving Biotechnology.* American Society of Microbiology. Washington, DC. pp. 133–140.
Ninfa,A., Reitzer,L. and Magasanik,B. (1987) *Cell*, **50**, 1039–1046.
Pereira,R., Ortuno,M. and Lawther,R. (1988) *Nucleic Acids Res.*, **16**, 5973–5989.
Prentki,P. and Krisch,H. (1984) *Gene*, **29**, 303–313.
Ptashne,M. (1988) *Nature*, **335**, 683–689.
Raibaud,O., Vidal–Ingigliardi,D. and Richet,E. (1989) *J. Mol. Biol.*, **205**, 471–485.
Ramos,J.L., Mermod,N. and Timmis,K.N. (1987) *Mol. Microbiol.*, **1**, 293–300.
Santero,E., Hoover,T., Keener,J. and Kustu,S. (1989) *Proc. Natl. Acad Sci. USA*, **86**, 7346–7350.
Sasse–Dwight,S. and Gralla,J. (1990) *Cell*, **62**, 945–954.
Silhavy,T., Berman,M.L. and Enquist,L.W. (1984) *Experiments with Gene Fusions.* Cold Spring Harbor Laboratory Press. Cold Spring Harbor, NY.
Snyder,U., Thompson,J.F. and Landy, A. (1989) *Nature*, **341**, 255–257
Thompson,R. and Mossig,G. (1988) *Nucleic Acids Res.*, **16**, 3313–3326.
Travers,A. (1990) *Cell*, **60**, 177–180.
Trifonov,E. (1985) *Crit. Rev. Biochem.*, **19**, 89–106
Yang, C. and Nash,H. (1989) *Cell*, **57**, 869–880.
Zaballos,A., Salas,M. and Mellado,R.P. (1987) *Gene*, **58**, 67–76.

Received on January 8, 1991; revised on January 30, 1991